

# Photoluminescence Studies on $\text{Eu}^{2+}$ -Activated $\text{Li}_2\text{SrSiO}_4$ —a Potential Orange-Yellow Phosphor for Solid-State Lighting

M. Pardha Saradhi and U. V. Varadaraju\*

Materials Science Research Centre and Department of Chemistry, Indian Institute of Technology Madras, Chennai 600036, India

Received June 12, 2006. Revised Manuscript Received September 1, 2006

A series of  $\text{Eu}^{2+}$ -activated  $\text{Li}_2\text{SrSiO}_4$  orange-yellow phosphor compositions exhibiting intense emission under 400–470 nm excitation are synthesized by solid-state reaction, and their luminescence properties are investigated as a function of activator concentration ( $\text{Eu}^{2+}$ ). The critical concentration is found to be 0.005 mol of  $\text{Eu}^{2+}$  ( $R_c = 34 \text{ \AA}$ ) per formula unit. The composition containing 0.005 mol of  $\text{Eu}^{2+}$  is also synthesized by a combustion technique followed by postannealing at different temperatures. The luminescence emission intensity of a combustion-synthesized sample increases with increasing annealing temperature. This is attributed to increased crystallinity and improved distribution of activator in the lattice in the combustion-synthesized sample. Attempts are made to develop white light-emitting diodes by combining an InGaN blue LED chip (420 nm) and a  $\text{Li}_2\text{SrSiO}_4:\text{Eu}^{2+}$  phosphor. Two distinct emission bands from the InGaN and  $\text{Li}_2\text{SrSiO}_4:\text{Eu}^{2+}$  (562 nm) are observed that combine to give a spectrum that appears white to the naked eye. The values of the CIE coordinates indicate that the  $\text{Li}_2\text{SrSiO}_4:\text{Eu}^{2+}$ -coated LED has improved red emission compared to the commercial YAG:Ce phosphor.

## Introduction

Considering the growing importance of energy savings and environmental friendliness, solid-state lighting (SSL) is emerging as a highly competent field and a possible alternative to existing lighting technologies. It is expected that white LEDs could replace incandescent bulbs because of numerous advantages such as higher energy efficiency, longer life and reliability, and a low temperature of performance. One approach to producing white light is the combination of blue LED with green-, yellow-, and red-emitting phosphor materials, viz. ZnS:Ag (blue), ZnS:Cu, Al (green), ZnCdS:Ag (red),<sup>1</sup> SrGa<sub>2</sub>S<sub>4</sub>:Eu<sup>2+</sup> (green), and ZnCdS:Ag,Cl (red).<sup>2</sup> This approach has a disadvantage, as it decreases the luminous efficiency due to absorption of the emitted photon from one phosphor by the other and sulfide-based materials also have low chemical stability. The most common way to produce white light is to combine a blue-emitting LED and a single oxide phosphor, which can be excited with blue light and gives a broad emission band covering the region from 500 to 600 nm.

In this regard, the first white LED that was fabricated has a combination of GaN LED and Y<sub>3</sub>Al<sub>5</sub>O<sub>12</sub>:Ce<sup>3+</sup> (YAG:Ce) yellow-emitting phosphor.<sup>3</sup> But this combination has a low color rendering index (CRI) of 75. In 1996, a white LED that had a combination of a blue LED chip and a yellow phosphor ((Y<sub>1-x</sub>Gd<sub>x</sub>)<sub>3</sub>(Al<sub>1-y</sub>Gd<sub>y</sub>)<sub>5</sub>O<sub>12</sub>:Ce<sup>3+</sup>) was commercialized.<sup>4</sup> Doping of Gd at the Y and Al sites improved<sup>5</sup> the

CRI to 85. The variation in  $x$  and  $y$  causes a shift in the YAG:Ce emission between 510 and 580 nm. Further improvement of CRI is possible only by doping an ion that can emit in the orange-red region or mixing of another red phosphor. An elegant solution lies in developing a new orange-yellow phosphor and combining it with a blue LED. Recently, oxynitride phosphors<sup>6,7</sup> have been given importance for generating white light, and efficient white LEDs have been reported by the combination of InGaN (460 nm) and orange-yellow oxynitride phosphors.<sup>8,9</sup> In this paper, we report a new orange-yellow phosphor that has a broad emission peak from yellow to orange-red with a broad excitation band.

In the present work, we synthesized and studied the optical properties of a  $\text{Eu}^{2+}$ -activated  $\text{Li}_2\text{SrSiO}_4$  orange-yellow phosphor and investigated the properties of white LEDs through the integration of the InGaN blue LED chip and the synthesized phosphor.  $\text{Li}_2\text{SrSiO}_4$  was first synthesized by Haferkorn et al.<sup>10</sup> using a sol–gel technique. In this paper, the compounds were synthesized by solid-state reaction (SSR) as well as combustion synthesis (CS).  $\text{Li}_2\text{SrSiO}_4$  crystallizes in a hexagonal system with space group  $P3_121$  and the structure refinement was done by taking  $\text{Li}_2\text{EuSiO}_4$  as the starting model. The synthesized phosphor was coated on an InGaN LED chip ( $\lambda_{\text{em}} = 420 \text{ nm}$ ) using standard LED

\* To whom correspondence should be addressed. Phone: 91-44-2257-4215. E-mail: varada@iitm.ac.in.

(1) Sato, Y.; Takahashi, N.; Sato, S. *Jpn. J. Appl. Phys.* **1996**, *35*, L838.  
 (2) Huh, Y. D.; Shim, J. H.; Kim, Y. H.; Do, Y. R. *J. Electrochem. Soc.* **2003**, *150* (2), H57–H60.  
 (3) Nakamura, S.; Fasol, G. *The Blue Laser Diode*; Springer: Berlin, 1996.  
 (4) Narukawa, Y. *Opt. Photonics News* **2004**, *15*, 24.

(5) Jüstel, T.; Nikol, H.; Ronda, C. *Angew. Chem., Int. Ed.* **1998**, *37*, 3084.  
 (6) Xie, R.-J.; Hirotsaki, N.; Mitomo, M.; Yamamoto, Y.; Suehiro, T.; Sakuma, K. *J. Phys. Chem. B* **2004**, *108* (32), 12027–12031.  
 (7) van Krevel, J. W. H.; van Rutten, J. W. T.; Mandal, H.; Hintzen, H. T. *J. Solid State Chem.* **2002**, *165*, 19–24.  
 (8) Li, Y. Q.; Delsing, C. A.; de With, G.; Hintzen, H. T. *Chem. Mater.* **2005**, *17*, 3242–3248.  
 (9) Xie, R.-J.; Hirotsaki, N.; Mitomo, M.; Takahashi, K.; Sakuma, K. *Appl. Phys. Lett.* **2006**, *88*, 101104–1.  
 (10) Haferkorn, B.; Meyer, G. Z. *Anorg. Allg. Chem.* **1998**, *624*, 1079.

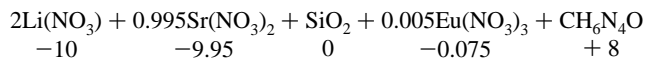
technology. The observed white emission is reported here and Commission Internationale de l'Éclairage (CIE) Chromaticity coordinates show better values compared to commercial YAG:Ce-coated LED.

## Experimental Section

**2.1. Synthesis.**  $\text{Li}_2\text{SrSiO}_4:\text{Eu}^{2+}$  compositions were synthesized by solid-state reaction (SSR) and combustion synthesis (CS) methods. The starting materials used were highly pure  $\text{SrCO}_3$  (Cerac, 99.99%),  $\text{Li}_2\text{CO}_3$  (Merck, 99.0%),  $\text{SiO}_2$  (Thermal Syndicate, 99.99%), and  $\text{Eu}_2\text{O}_3$  (Indian Rare Earths, 99.9%). For combustion synthesis, the metal oxides/carbonates were dissolved in  $\text{HNO}_3$  (analytical reagent) to obtain the corresponding nitrates; commercial fumed silica of grain size  $\sim 10$  nm (CABOT Sanmar Ltd. India, 99.9%) is used as the source of Si, and carbonylhydrazide ( $\text{CH}_6\text{N}_4\text{O}$ ; Sigma–Aldrich, 98.0%) was used as the fuel. Excess  $\text{Li}_2\text{CO}_3$  was taken in order to compensate for the  $\text{Li}_2\text{O}$  evaporation. The amount of  $\text{Li}_2\text{CO}_3$  needed was optimized by X-ray diffraction (XRD) and photoluminescence (PL) studies.

**2.1.1. Solid-State Reaction (SSR).** Stoichiometric amounts of starting materials were ground well and preheated at  $600^\circ\text{C}$  for 12 h in order to avoid lithium volatilization. After the pre-heat treatment, the obtained product was ground well and placed in an alumina boat inside a tubular furnace and heated slowly to  $800^\circ\text{C}$  under a reducing atmosphere (5%  $\text{H}_2$  + 95%  $\text{N}_2$ ). The sample was kept at this temperature for 12 h and then cooled to room temperature. Gas flow was maintained until the furnace was cooled to room temperature.

**2.1.2. Combustion Synthesis (CS).** From the literature, we find that fumed  $\text{SiO}_2$  was used as a silica source for combustion synthesis; there are a few reports on combustion synthesis of silicate host lattices.<sup>11</sup> For the calculation of oxidizer to fuel ratio, the elements are assigned formal valences as follows:  $\text{Li} = +1$ ,  $\text{Sr} = +2$ ,  $\text{Eu} = +3$ ,  $\text{C} = +4$ ,  $\text{N} = 0$ ,  $\text{O} = -2$  and  $\text{H} = +1$ . Accordingly, the oxidizer and fuel values for the various reactants are as given below



For complete combustion, the oxidizer/fuel ratio should be equal to 1. Thus, the molar ratio of the reactants taken is 2:0.995:0.005:1:2.5  $\text{LiNO}_3:\text{Sr}(\text{NO}_3)_2:\text{Eu}(\text{NO}_3)_3:\text{SiO}_2:\text{CH}_6\text{N}_4\text{O}$ . The mixture was taken in a glass beaker and stirred until a slurry resulted. The beaker was kept in a preheated furnace at  $550^\circ\text{C}$ . Within a few minutes, the slurry boiled and was ignited to produce a self-propagating flame. The product obtained was postannealed in a reducing atmosphere (5%  $\text{H}_2$  + 95%  $\text{N}_2$ ) at various temperatures, viz.  $600^\circ\text{C}/3$  h,  $800^\circ\text{C}/3$  h and  $800^\circ\text{C}/12$  h.

**2.2. Characterization.** The powder X-ray diffraction patterns (XRD) were recorded in the  $2\theta$  range  $5$ – $90^\circ$  using a Philips X'pert diffractometer with Bragg–Brentano geometry. Structure refinement was carried out by the Rietveld method using the FullProf program.<sup>12</sup> The reflectance spectra of samples were recorded using a UV–visible spectrophotometer with a 150 mm integrating sphere attachment (V-560, JASCO) with  $\text{BaSO}_4$  as reference. The room-temperature photoluminescence (PL) spectra were recorded using a spectrofluorometer operating in the range  $220$ – $720$  nm (FP-6500, JASCO). CIE Chromaticity coordinates were calculated using emission

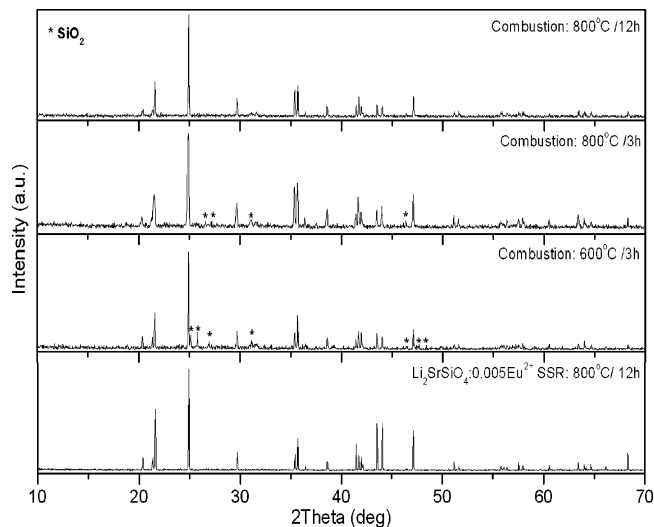


**Figure 1.** Powder X-ray diffraction patterns of  $\text{Li}_2\text{SrSiO}_4:0.005\text{Eu}^{2+}$  synthesized by solid-state reaction and combustion methods. The patterns of combustion-synthesized samples annealed at various temperatures are shown.

spectra.<sup>13</sup> InGaN LED chips supported on SiC substrate were used for coating the phosphors. The fluorescence decay measurements of samples were carried out using the time correlated single photon counting technique (model 5000 U, IBH, U.K.) with a microchannel plate photo multiplier tube (Hamamtsu R3809U) and blue LED chip ( $\lambda_{\text{max}} = 455$  nm) as the excitation source; data collection was carried out by the software (Datastation 2000) provided by IBH.

## Results and Discussion

**3.1. Phase Formation.** The following compositions were synthesized by SSR in the present study with a 5 mol % excess of  $\text{Li}_2\text{CO}_3:\text{Li}_2\text{Sr}_{1-x}\text{Eu}_x\text{SiO}_4$ ,  $x = 0, 0.0025, 0.005, 0.0075, 0.01, 0.02, 0.03, 0.04$ , and  $0.05$ . All compositions were single phase. The representative powder XRD patterns of  $\text{Li}_2\text{SrSiO}_4:0.005\text{Eu}$  synthesized by SSR are shown in Figure 1. Figure 1 also shows powder XRD patterns of samples synthesized by the CS method without excess  $\text{Li}_2\text{CO}_3$ . The as-combusted sample has a major phase with the  $\text{Li}_2\text{SrSiO}_4$  structure along with  $\text{SiO}_2$  as a minor second phase. The second phase is progressively eliminated, and single phase  $\text{Li}_2\text{Sr}_{0.995}\text{SiO}_4:0.005\text{Eu}^{2+}$  is achieved with an increase in postannealing temperature/time. We have also synthesized compounds with excess  $\text{Li}_2\text{CO}_3$  using the CS technique. We compared the phase formation with materials synthesized by CS without an excess of  $\text{Li}_2\text{CO}_3$ . We observed that there is no difference in the phase formation behavior with or without excess  $\text{Li}_2\text{CO}_3$ . We attribute this to the short reaction time during combustion wherein volatilization of  $\text{Li}_2\text{O}$  is negligible. It is possible  $\text{Li}_2\text{O}$  would react with other components in the reaction mixture, forming a matrix, and lithium volatilization from the precursor matrix is not significant during subsequent heating. It is to be emphasized that  $\text{Li}_2\text{O}$  is volatile, but  $\text{Li}^+$  present in other matrices does not have significant volatilization.

All the reflections are indexed on the basis of a hexagonal unit cell of  $\text{Li}_2\text{EuSiO}_4$  (JCPDS no. 47-0120). In order to optimize the amount of excess  $\text{Li}_2\text{CO}_3$  used in SSR, we

(11) Gonzalez-Ortega, J. A.; Tejada, E. M.; Perea, N.; Hirata, G. A.; Bosze, E. J.; Mckittrick, J. *Opt. Mater.* **2005**, *27*, 1221.

(12) Rodríguez-Carvajal, J. *An Introduction to the Program FullProf 2000*; Laboratoire Léon Brillouin, CEA-CNRS: Saclay, France, 2001.

(13) Hunt, R. W. G. *The Reproduction of Color in Photography, Printing & Television*; Fountain Press: London, 1987.

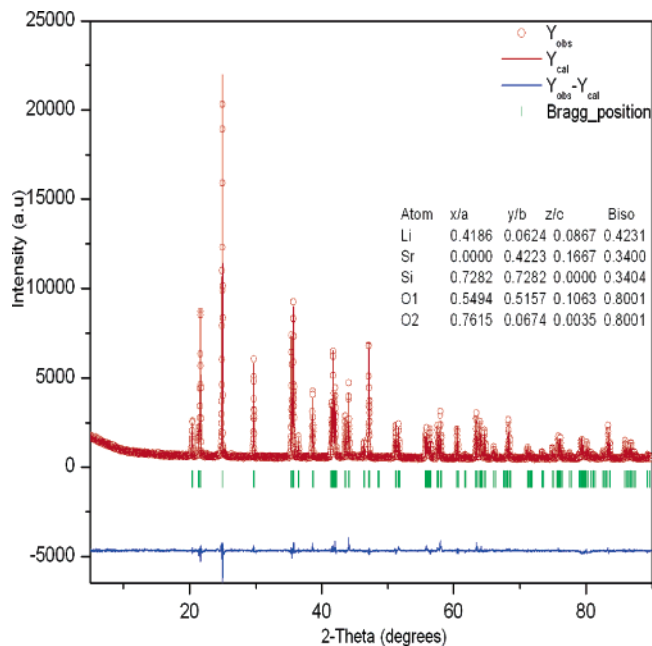


**Figure 2.** Rietveld refinement plot of X-ray diffraction data for Li<sub>2</sub>SrSiO<sub>4</sub>. Observed, calculated, and difference profiles are plotted on the same scale. The atomic positions of Li<sub>2</sub>SrSiO<sub>4</sub> are given.

synthesized Li<sub>2</sub>SrSiO<sub>4</sub>:0.01Eu<sup>2+</sup> with 0, 5, and 10 mol % excess Li<sub>2</sub>CO<sub>3</sub>, referred to as samples A, B, and C, respectively. No crystalline impurity phase could be detected in any of the three samples.

The crystal structure refinement of Li<sub>2</sub>SrSiO<sub>4</sub> was done by taking Li<sub>2</sub>EuSiO<sub>4</sub> as the starting model with space group *P*3<sub>1</sub>21. The observed, calculated, and difference patterns are shown in Figure 2. The obtained profile factors are:  $R_p = 4.74$ ,  $R_{wp} = 6.12$ ,  $R_{exp} = 3.56$ , and  $\chi^2 = 2.95$ , revealing the good quality of fitting. The refined lattice parameters are  $a = 5.023(5)$  Å and  $c = 12.457(1)$  Å, which match well with those reported in the literature.<sup>10</sup> Sr<sup>2+</sup> is coordinated to eight oxygens with Sr–O bond distances of 2.720 Å (×2), 2.621 Å (×2), 2.555 Å (×2), and 2.536 Å (×2). Li<sup>+</sup> is coordinated to four oxygens with Li–O bond distances of 2.01, 1.978, 1.941, and 1.840 Å. Si<sup>4+</sup> is coordinated to four oxygens with Si–O bond distances of 1.722 Å (×2) and 1.664 Å (×2).

**3.2. Diffuse Reflectance Spectra.** The diffuse reflectance spectra of Li<sub>2</sub>Sr<sub>1-x</sub>Eu<sub>x</sub>SiO<sub>4</sub>,  $x = 0.01–0.05$  in steps of 0.01, are given in Figure 3. Two strong absorption bands are present at 260 and 400, and one more weak absorption band is observed at 310 nm; all the bands are attributed to the  $4f^7 \rightarrow 4f^65d^1$  electronic transitions of Eu<sup>2+</sup>. These bands are absent in the DRS spectrum of the parent phase (unsubstituted Li<sub>2</sub>SrSiO<sub>4</sub>). The band at 220 nm observed for all compositions is due to host absorption. The same is seen for the parent phase (not shown in the figure).

**3.3. Photoluminescence of Li<sub>2</sub>SrSiO<sub>4</sub>:Eu<sup>2+</sup>.** The PL excitation spectrum of Li<sub>2</sub>SrSiO<sub>4</sub>:0.005Eu<sup>2+</sup> is shown in Figure 4. The spectrum clearly indicates an absorption band at 308 nm and broad absorption from 400 to 470 nm. All the excitation bands are due to  $4f^7 \rightarrow 4f^65d^1$  transitions, and the broad excitation from 400 to 470 nm matches well with LED (GaN-based) emission. The photoluminescence emission spectra of the three samples with different Li<sub>2</sub>CO<sub>3</sub> contents (A, B, and C) are given in Figure 5. The maximum

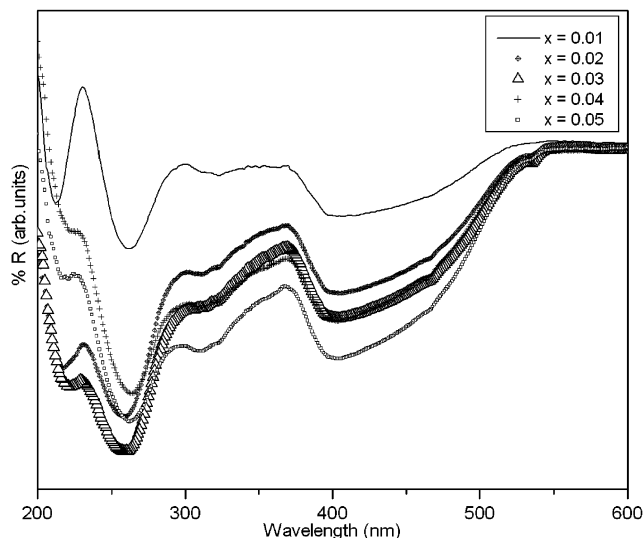


**Figure 3.** Diffuse reflectance spectra of Li<sub>2</sub>Sr<sub>1-x</sub>Eu<sub>x</sub>SiO<sub>4</sub> ( $x = 0.01–0.05$  in steps of 0.01).

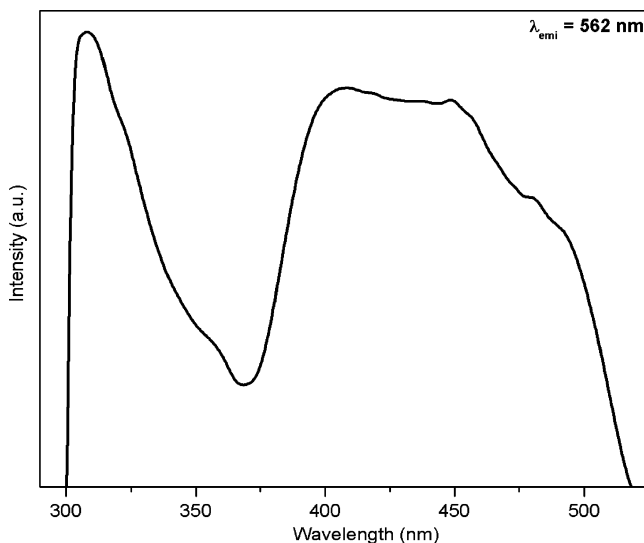


**Figure 4.** Photoluminescence excitation spectrum of Li<sub>2</sub>SrSiO<sub>4</sub>:0.005Eu<sup>2+</sup>.

PL emission intensity is observed for sample B when compared to samples A and C. This can be explained as follows: in the case of sample A, there can be lithium ion vacancies in the lattice due to lithium oxide evaporation during synthesis. These vacancies can act as trapping centers, which leads to a decrease in emission intensity. In comparison, sample B synthesized with 5 mol % excess Li<sub>2</sub>CO<sub>3</sub> to compensate for the loss in Li<sub>2</sub>O is expected to be devoid of Li<sup>+</sup> vacancies and hence has significantly higher emission intensity. In the case of sample C, the presence of a considerable excess of second-phase amorphous Li<sub>2</sub>O dilutes the matrix, and therefore, the emission intensity is apparently marginally lowered. The existence of traps in the lattice is further confirmed by fluorescence lifetime measurements. The observed lifetimes are as follows: sample A,  $\tau = 30$  ns, 0.68 μs; sample B,  $\tau = 0.80$  μs; and sample C,  $\tau = 1.1$  μs. From the values of the lifetime, it is clear that sample A has two types of traps. The  $\tau = 30$  ns trap may be due to the existence of lithium ion vacancies in the lattice. The single value for each of the other two samples indicates the absence of lithium ion vacancies in the lattice in these samples.

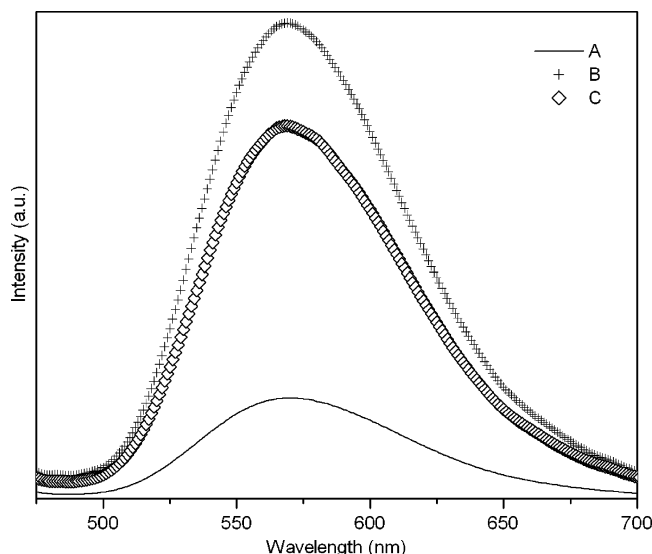


**Figure 5.** Photoluminescence emission spectra of  $\text{Li}_2\text{Sr}_{0.99}\text{Eu}_{0.01}\text{SiO}_4$  with (A) 0, (B) 5, and (C) 10 mol % excess  $\text{Li}_2\text{CO}_3$ .

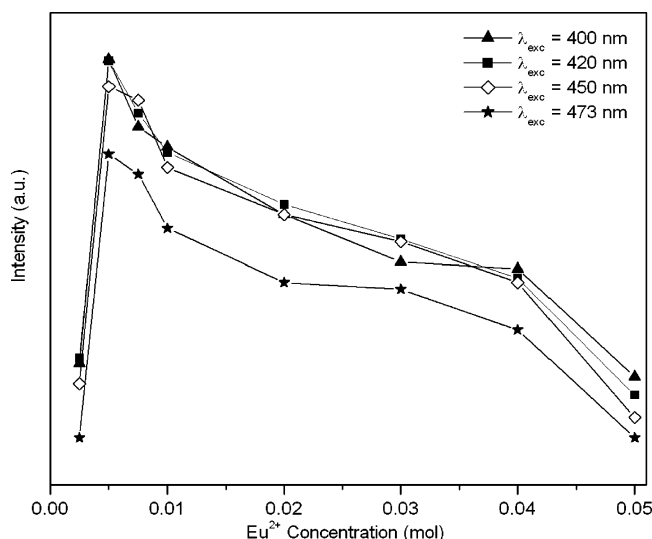


**Figure 6.** Emission intensities of  $\text{Eu}^{2+}$  fluorescence as a function of  $\text{Eu}^{2+}$  concentration in  $\text{Li}_2\text{SrSiO}_4:\text{Eu}^{2+}$ . Emission intensities were measured at 400, 420, 450, and 473 nm excitation.

As it has a broad excitation, this phosphor can be excited with different wavelengths. The phosphor compositions show a strong orange-yellow emission band with a maximum at 562 nm extending to 650 nm. The emission intensity is almost equal under 400, 420, and 450 nm excitations. This feature makes these phosphor compositions very attractive for application in LEDs. The emission intensity corresponding to the 473 nm excitation is lower compared to that of others. This is due to the relatively lower absorption at this wavelength (Figure 4).

The emission intensities of  $\text{Li}_2\text{SrSiO}_4:\text{Eu}^{2+}$  phases as a function of  $\text{Eu}^{2+}$  concentration at different excitation wavelengths are shown in Figure 6. With increasing concentration of  $\text{Eu}^{2+}$ , the emission intensity increases up to 0.005 mol of  $\text{Eu}^{2+}$ ; a further increase in the  $\text{Eu}^{2+}$  concentration leads to a decrease in the emission intensity, which is an indication of nonradiative energy transfer between  $\text{Eu}^{2+}$  ions. This may occur because of exchange interaction, radiation reabsorption, or multipole–multipole interaction.<sup>14</sup> The optical transitions in  $\text{Li}_2\text{SrSiO}_4:\text{Eu}^{2+}$  are allowed ( $4f^7 \rightarrow 4f^65d^1$ ), and hence

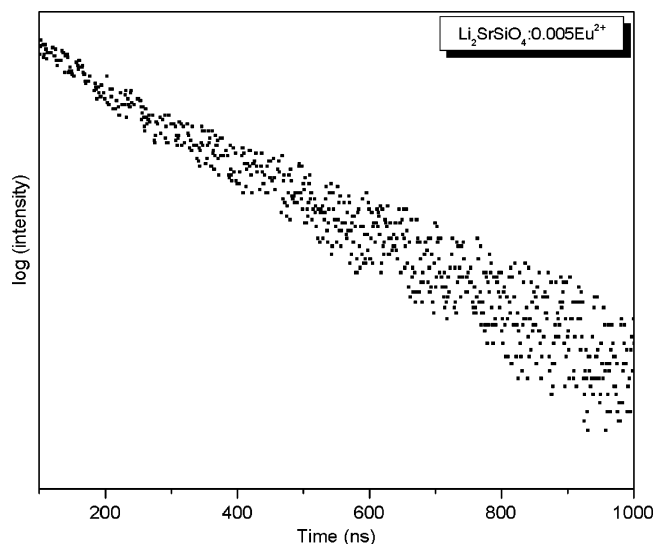


**Figure 7.** Representative fluorescence decay curves of the 562 nm emission band of  $\text{Li}_2\text{SrSiO}_4:0.005\text{Eu}^{2+}$ .

exchange interactions are ruled out. In the present case, radiation reabsorption due to spectral overlap alone cannot be fully responsible for nonradiative energy transfer between the  $\text{Eu}^{2+}$  ions. Hence, the process of energy transfer should be electric multipole–multipole interaction. The probability of energy transfer between the  $\text{Eu}^{2+}$  ions due to multipole–multipole interaction is distance-dependent.<sup>15,16</sup> As the concentration of  $\text{Eu}^{2+}$  ions increases, the distance between the  $\text{Eu}^{2+}$  ions becomes smaller, leading to the high probability of energy transfer among the  $\text{Eu}^{2+}$  ions. From Figure 6, it is clear that 0.005 mol is the critical concentration of  $\text{Eu}^{2+}$ . A rough estimation of the critical distance ( $R_c$ ) for energy transfer can be made using the relation given by Blasse<sup>17</sup>

$$R_c \approx 2 \left[ \frac{3V}{4\pi x_c Z} \right]^{1/3} \quad (1)$$

where  $V$  is the volume of the unit cell,  $x_c$  is the critical concentration of the activator ion, and  $Z$  is the number of formula units per unit cell. For the  $\text{Li}_2\text{SrSiO}_4$  host,  $Z = 3$ ,  $x_c = 0.005$ , and  $V = 315 \text{ \AA}^3$ . Using these values, the obtained  $R_c$  value is  $\approx 34 \text{ \AA}$ . This large value of  $R_c$  can be attributed to the small Stokes shift ( $1218 \text{ cm}^{-1}$ ) resulting from the stiffness of the host lattice, which is made of an  $\text{SiO}_4$  tetrahedral network and spectral overlap between the emission and excitation bands.<sup>18</sup> Figure 7 shows representative fluorescence decay curves of the 562 nm emission band for  $\text{Li}_2\text{Sr}_{0.995}\text{Eu}_{0.005}\text{SiO}_4$ . As described by Blasse and Grabmaier,<sup>15</sup> it is well-known that the decay behavior can be expressed as follows

$$I = I_0 \exp(-t/\tau) \quad (2)$$

where  $I_0$  and  $I$  are the luminescence intensities at time 0 and  $t$ , respectively, and  $\tau$  is the luminescence lifetime. Using eq

(14) Van Uitert, L. G. *J. Electrochem. Soc.* **1967**, *114*, 1048.

(15) Blasse, G.; Grabmaier, B. C. *Luminescent Materials*; Springer-Verlag: Berlin, 1994.

(16) Dexter, D. L. *J. Chem. Phys.* **1953**, *21*, 836–850.

(17) Blasse, G. *Philips Res. Rep.* **1969**, *24*, 131.

(18) Lucas, F.; Jaulmes, S.; Querton, M. *J. Solid State Chem.* **2000**, *150*, 404–409.

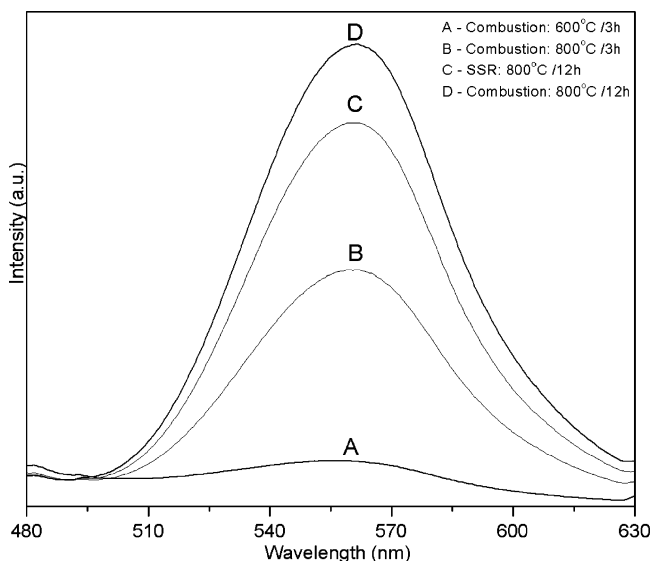


**Figure 8.** Photoluminescence emission spectra of Li<sub>2</sub>Sr<sub>0.995</sub>SiO<sub>4</sub>:0.005Eu<sup>2+</sup> synthesized by solid-state reaction and combustion methods. The spectra of CS samples postannealed at various temperatures are shown.

2, we found the values of the lifetime of the excited-state in Li<sub>2</sub>Sr<sub>1-x</sub>Eu<sub>x</sub>SiO<sub>4</sub> for  $x = 0.0025, 0.005, 0.0075,$  and  $0.01-0.05$  to be 0.90, 1.10, 0.90, 0.80, 0.78, 0.75, 0.70, and 0.63  $\mu$ s, respectively. Above the critical concentration ( $x_c = 0.005$ ), the lifetime values decrease monotonously with increasing concentration of the dopant ion. Thus, at high concentrations of Eu<sup>2+</sup>, the migration of energy nonradiatively between the Eu<sup>2+</sup> increases, resulting in a decrease in the lifetime.

The technique of combustion synthesis (CS) can be used to synthesize phosphors at low sintering temperature with high purity, high chemical homogeneity, and nanoparticle size.<sup>20,21</sup> The best composition, Li<sub>2</sub>SrSiO<sub>4</sub>:0.005Eu<sup>2+</sup>, was also synthesized by the CS technique; the optical properties of the samples were compared with those of the samples synthesized by SSR. The PL emission spectra of SSR and CS samples are shown in Figure 8. The emission intensity of the CS sample increases with an increase in postannealing temperature/time. The highest emission intensity is obtained for the sample postannealed at 800 °C for 12 h, which is higher than that of the sample synthesized by SSR. This can be attributed to improved crystallinity and a higher degree of homogeneity of the activator in the sample synthesized by CS. We compared the photoluminescence properties with those of materials synthesized by CS without an excess of Li<sub>2</sub>CO<sub>3</sub>. We observed that there is no change in the properties with or without excess Li<sub>2</sub>CO<sub>3</sub> (section 3.1).

The CIE values for the YAG:Ce phosphor are  $x = 0.3228,$   $y = 0.6208$  and those of Li<sub>2</sub>SrSiO<sub>4</sub>:0.005Eu presently studied are  $x = 0.3677,$   $y = 0.5148$ . LEDs were fabricated by mixing the Li<sub>2</sub>SrSiO<sub>4</sub>:0.005Eu<sup>2+</sup> phosphor with a transparent epoxy resin and coating on InGaN LED chip ( $\lambda_{\text{max}} = 420$  nm). The coated chip was kept in a centrifuge for about 30 min in

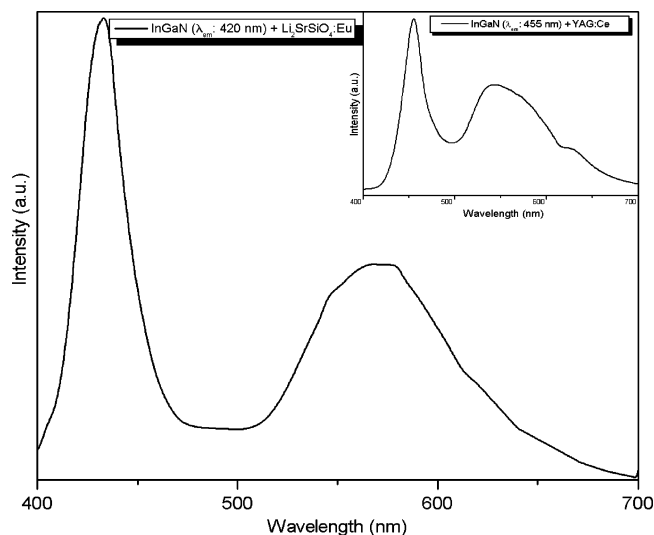


**Figure 9.** Photoluminescence spectrum of LED fabricated using an InGaN-based LED chip and Li<sub>2</sub>Sr<sub>0.995</sub>SiO<sub>4</sub>:0.005Eu<sup>2+</sup> phosphor. Inset shows the same for a commercial YAG:Ce phosphor.

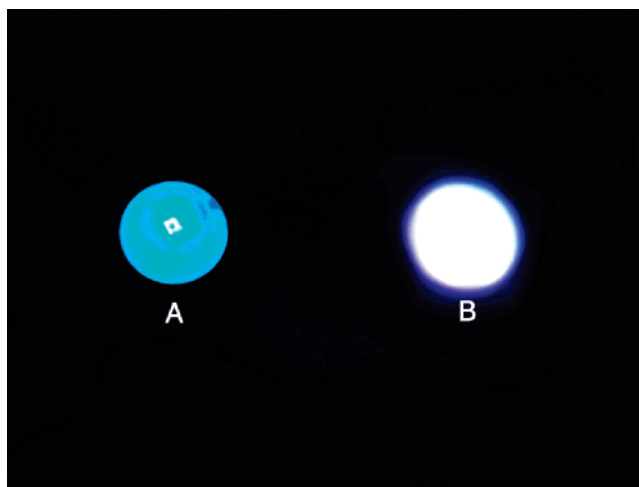


**Figure 10.** Photographs of (A) InGaN blue LED chip and (B) InGaN LED chip coated with Li<sub>2</sub>SrSiO<sub>4</sub>:0.005Eu<sup>2+</sup>.

order to remove any air bubbles and the resin was subsequently cured in an air oven. The PL emission spectrum recorded on the coated LED is shown in Figure 9; the inset shows the same for the commercial YAG:Ce phosphor-coated LED ( $\lambda_{\text{max}} = 455$  nm) in the present study, for comparison. The CIE chromaticity coordinates of YAG:Ce-coated LED calculated from the PL spectra are (0.3069,0.3592), and the values match well with values reported in the literature.<sup>22</sup> The chromaticity coordinates of Li<sub>2</sub>SrSiO<sub>4</sub>:0.005Eu<sup>2+</sup>-coated LED are (0.3346,0.3401). The CIE values of Li<sub>2</sub>SrSiO<sub>4</sub>:Eu<sup>2+</sup> indicate that the red component is improved vis a vis YAG:Ce, which would help in increasing the CRI. The luminous efficiency of the Li<sub>2</sub>SrSiO<sub>4</sub>:0.005Eu<sup>2+</sup> LED is 35 lm/W and is comparable to that of YAG:Ce (around 35 lm/W). The InGaN LED chip before and after coating with the Li<sub>2</sub>SrSiO<sub>4</sub>:0.005Eu<sup>2+</sup> phosphor is shown in Figure 10. These results reveal that the phosphor Li<sub>2</sub>Sr<sub>0.995</sub>SiO<sub>4</sub>:0.005Eu<sup>2+</sup> is suitable for generating bright white emission under 420 nm excitation.

(19) Blasse, G.; Grabmaier, B. C. *Luminescent Materials*; Springer-Verlag: Berlin, 1994; p 96.

(20) Kingsley, J. J.; Suresh, K.; Patil, K. C. *J. Mater. Sci.* **1990**, 25, 1305–1312.

(21) Ekambaram, S.; Patil, K. C.; Maaza, M. *J. Alloys Compd.* **2004**, 393, 81–92.

(22) Park, J. K.; Kim, C. H.; Park, S. H.; Park, H. D.; Choi, S. Y. *Appl. Phys. Lett.* **2004**, 84, 1647.

### Conclusions

$\text{Li}_2\text{SrSiO}_4$  is synthesized by SSR and CS methods and structure refinement is carried out. The optical properties of  $\text{Eu}^{2+}$ -doped  $\text{Li}_2\text{SrSiO}_4$  are studied. The phosphors have broad excitation band (400–470 nm) with orange-yellow emission (562 nm). The variation of Eu concentration in the lattice was studied in order to find out the critical concentration ( $x_c$ ) and distance ( $R_c$ ). The mechanism of concentration quenching of  $\text{Eu}^{2+}$  in  $\text{Li}_2\text{SrSiO}_4$  is confirmed to be dipole–dipole interaction. The emission intensity of the CS sample increases with increasing annealing temperature/time and is higher than that of the corresponding SSR-synthesized composition because of improved crystallinity and homogeneity. Further, we attempted to develop white LEDs by

integrating the InGaN blue LED chip and  $\text{Li}_2\text{SrSiO}_4:0.005\text{Eu}^{2+}$  phosphor. The combination of a blue-emitting LED (420 nm) and orange-yellow phosphor results in white light and the CIE values are better than those of the YAG:Ce phosphor coated LED (455 nm).  $\text{Li}_2\text{SrSiO}_4:\text{Eu}^{2+}$  is a potential phosphor for SSL lighting using InGaN (420 nm) to produce white light.

**Acknowledgment.** M.P.S. acknowledges the National Centre for Ultrafast Processes, University of Madras, for help with fluorescence lifetime measurements and Dr. N. Lakshminarasimhan for suggesting the system and useful discussions.

CM061362U